Biosensors and Bioelectronics 233 (2023) 115339

Contents lists available at ScienceDirect

Biosensors and Bioelectronics

journal homepage: www.elsevier.com/locate/bios

Homogeneous immunoassay for cyclopiazonic acid based upon mimotopes and upconversion-resonance energy transfer

Fernando Pradanas-González [a], Riikka Peltomaa [b], Satu Lahtinen [b], Álvaro Luque-Uría [a], Vicente Más [c], Rodrigo Barderas [c], Chris M. Maragos [d], Ángeles Canales [e], Tero Soukka [b,**], Elena Benito-Peña [a,*], María C. Moreno-Bondi [a,1]

[a] Department of Analytical Chemistry, Faculty of Chemistry, Complutense University of Madrid, Ciudad Universitaria, 28040, Madrid, Spain
[b] Department of Life Technologies/Biotechnology, University of Turku, Kiinamyllynkatu 10, 20520, Turku, Finland
[c] Instituto de Salud Carlos III, Ctra. Majadahonda-Pozuelo, 28220, Madrid, Spain
[d] Mycotoxin Prevention and Applied Microbiology Research Unit, National Center for Agricultural Utilization Research, Agricultural Research Service, USDA, 1815 N University, Peoria, IL, 61604, USA
[e] Department of Organic Chemistry, Faculty of Chemistry, Complutense University of Madrid, Ciudad Universitaria, 28040, Madrid, Spain

ARTICLE INFO

The authors would like to dedicate this publication to the late Prof. María C. Moreno-Bondi who passed away prior to the submission of the research paper. Her impact on science will continue to be felt through her effect on us.

Keywords:
Cyclopiazonic acid
Mimotope
Upconversion nanoparticle
Förster resonance energy transfer
Immunoassay
Food control

ABSTRACT

Strains of *Penicillium* spp. are used for fungi-ripened cheeses and *Aspergillus* spp. routinely contaminate maize and other crops. Some of these strains can produce toxic secondary metabolites (mycotoxins), including the neurotoxin α-cyclopiazonic acid (CPA). In this work, we developed a homogeneous upconversion-resonance energy transfer (UC-RET) immunoassay for the detection of CPA using a novel epitope mimicking peptide, or mimotope, selected by phage display. CPA-specific antibody was used to isolate mimotopes from a cyclic 7-mer peptide library in consecutive selection rounds. Enrichment of antibody binding phages was achieved, and the analysis of individual phage clones revealed four different mimotope peptide sequences. The mimotope sequence, ACNWWDLTLC, performed best in phage-based immunoassays, surface plasmon resonance binding analyses, and UC-RET-based immunoassays. To develop a homogeneous assay, upconversion nanoparticles (UCNP, type $NaYF_4$:Yb^{3+}, Er^{3+}) were used as energy donors and coated with streptavidin to anchor the synthetic biotinylated mimotope. Alexa Fluor 555, used as an energy acceptor, was conjugated to the anti-CPA antibody fragment. The homogeneous single-step immunoassay could detect CPA in just 5 min and enabled a limit of detection (LOD) of 30 pg mL^{-1} (1.5 μg kg^{-1}) and an IC_{50} value of 0.36 ng mL^{-1}. No significant cross-reactivity was observed with other co-produced mycotoxins. Finally, we applied the novel method for the detection of CPA in spiked maize samples using high-performance liquid chromatography coupled to a diode array detector (HPLC-DAD) as a reference method.

1. Introduction

With the blooming of nanotechnology, many efforts have been made to develop nanomaterials to serve as optical probes in biosensing applications and improve the sensitivity of the assays. Their use for mycotoxin detection has been no exception (Farka et al., 2017; Fu et al., 2017). A wide variety of nanoprobes, such as metal and metal oxide nanoparticles, silicon nanomaterials, quantum dots (QDs), persistent luminescence nanoparticles, metal nanoclusters, metal-organic frameworks and upconversion nanoparticles (UCNPs) (Lin et al., 2022), have been applied for the analysis of mycotoxins. All these nanomaterials present high surface-to-volume ratios and a wide variety of surface decoration possibilities that allow their functionalization with different bio-recognition elements, making them very suitable for their application in biosensors (Fu et al., 2017).

UCNPs consist of an inorganic crystalline host lattice, usually $NaYF_4$, doped with two lanthanide ions (*i.e.*, sensitizer and activator, such as Yb^{3+} and Er^{3+}, respectively) responsible for the upconversion process

* Corresponding author.
** Corresponding author.
E-mail addresses: tejoso@utu.fi (T. Soukka), elenabp@ucm.es (E. Benito-Peña).
[1] The late.

https://doi.org/10.1016/j.bios.2023.115339
Received 26 November 2022; Received in revised form 6 April 2023; Accepted 17 April 2023
Available online 19 April 2023

(Dong et al., 2015). These nanoparticles have a photophysical feature whereby they convert low energy near-infrared (NIR) radiation into higher energy radiation, typically in the ultraviolet–visible range. This unique anti-Stokes shift enables the total elimination of auto-fluorescence, which is the most important feature to improve the sensitivity and reduce the possible optical interferences from the sample matrix (Peltomaa et al., 2021). In addition, UCNPs exhibit high biocompatibility as well as chemical and thermal photo-stability, making them suitable for conjugation with targeting ligands (Ansari et al., 2021). Due to their superior photochemical properties, UCNPs have also been used as energy donors in upconversion-resonance energy transfer (UC-RET) based biosensing systems since they can overcome the toxicity limitation of other nanomaterials commonly used as energy donors, such as QDs (Ansari et al., 2021). UCNPs have emerged as a promising alternative for food analysis (Peltomaa et al., 2021) and have been applied to control various contaminants like pesticides, heavy metal ions, antibiotics, estrogens, pathogenic bacteria, and mycotoxins (Abdul Hakeem et al., 2021). In addition to the potential of high sensitivity, the mix-and-measure type homogeneous UC-RET based assays render analyses rapid and simple to perform. Many UC-RET-based detection strategies rely on the use of nanomaterial-based acceptors, such as gold nanoparticles, and the measurement of upconversion quenching (Ansari et al., 2021), but the use of molecular fluorescent dyes as acceptors is preferrable from both a kinetic and steric hindrance point of view. Furthermore, the sensitized measurement of acceptor emission rather than the donor quenching can avoid the challenges observed when complete quenching of UCNP emission occurs (Rantanen et al., 2008). Nevertheless, the rapid implementation of UCNP-based detection strategies in routine diagnostics and bioanalytical applications (Gorris and Resch-Genger, 2017; Wilhelm, 2017) relies on the availability of commercial microplate fluorometers to integrate a near-infrared diode laser excitation allowing dedicated photon upconversion luminescence readout. The current bottleneck would be alleviated by boosting the entry of these instruments into the market.

Cyclopiazonic acid (CPA) is an indole-tetramic acid mycotoxin produced as a secondary metabolite by several *Penicillium* and *Arpergillus* fungal species. CPA can occur naturally in food commodities of animal origins, such as milk and cheese, and of plant origin, such as peanuts, wheat, rice, or figs (Ostry et al., 2018). CPA has also been reported in maize samples (Hossain et al., 2019; Maragos et al., 2017), which is one of the most widely consumed cereals in the world due to its nutritional properties and potential health benefits (Rouf Shah et al., 2016). A variety of reports have demonstrated that CPA elicits toxic effects in both animals and human cells (Hymery et al., 2014; Ostry et al., 2018). The co-occurrence of CPA with other mycotoxins of more significant impact, such as aflatoxins, has hindered the studies of this emerging toxin ever since its discovery back in 1968. When CPA is co-administered with aflatoxins, a toxic synergistic effect has been observed and, although the mechanism is not yet clear, it demonstrates the toxicity of this mycotoxin (Burdock and Flamm, 2000; Ostry et al., 2018; Ma et al., 2022). Currently there are no maximum residue limits or guidelines for CPA in foodstuffs, but it is considered a toxic compound for humans, with an acceptable daily intake (ADI) of 10 μg/kg/day (Burdock and Flamm, 2000) or 0.1 μg/kg/day (De Waal, 2002), and therefore, it is highly important to detect CPA in order to ensure safe food consumption.

Conventionally, analysis of mycotoxins has been conducted by liquid chromatography (LC) coupled to different detectors. In particular, CPA has been analyzed by LC coupled to diode array detectors (DAD) (Aresta et al., 2003; Motta and Soares, 2001), tandem mass spectrometry (Ansari and Häubl, 2016; Vulić et al., 2021; Wang et al., 2022) and even fluorescence detectors after photolysis (Soares et al., 2010). Although these techniques are accurate and sensitive, the high cost of the instrumentation and maintenance, the need for skilled personnel, and the multi-step and time-consuming clean-up and extraction protocols pose a disadvantage for their application. Alternatively, biosensors and bioanalytical methods have proven to be a cost-effective option for the rapid screening of mycotoxins. These methods can be integrated into simple testing devices overcoming the limitations of conventional chromatographic techniques (Jia et al., 2021). Immunoassays are one of the most widespread biosensor-based methodologies due to the high specificity of the antibody–antigen interaction and the fast response time. Different immunoassays have been employed for the analysis of CPA, such as imaging surface plasmon resonance (Hossain et al., 2019), lateral flow immunoassays (Hu et al., 2021; Li et al., 2020) and, to a greater extent, enzyme-linked immunosorbent assays (ELISA) (Hahnau and Weiler, 1991, 1993; Huang and Chu, 1993; Maragos et al., 2017; Yu and Chu, 1998). All these approaches are based on competitive assay formats, in which CPA is conjugated to a carrier protein to allow its immobilization or a tracer that enables its direct detection. Although competitive immunoassays are the most common approach for the analysis of low-molecular weight molecules, the synthesis of toxin conjugates is one of the major limitations of this assay format. The handling of toxic substances poses a risk to the operator, and the synthesis tends to be challenging and time-consuming. Batch-to-batch variations can even result in an alteration of the epitope and thus have an effect on the antibody binding (Peltomaa et al., 2018b).

An alternative to overcome these drawbacks is the use of epitope-mimicking peptides, also known as mimotopes. These bioinspired elements are peptides that mimic the epitope and can compete with the analyte for antibody binding in competitive assays (Huang et al., 2021). Mimotopes are commonly isolated from phage-displayed peptide libraries (Peltomaa et al., 2019b), and several phage-based immunoassays have been applied for the analysis of a wide variety of mycotoxins (He et al., 2014; Hou et al., 2019; Wang et al., 2013; Yan et al., 2019). Novel phage-free mimotope-based approaches have been reported to refrain from the use of viruses, which can make the assay difficult due to their large size (Peltomaa et al., 2016) and also the safety concern associated with their biologically active nature (Smartt and Ripp, 2011). Different mimotopes-based immunoassays have been implemented demonstrating that peptide mimetics are functional when used alone (Huang et al., 2021). In fact, with phage-free immunoassay it has been possible to obtain better sensitivities than with phage-borne peptides, whether recombinant peptide fusion proteins (Luque-Uría et al., 2021; Peltomaa et al., 2018a) or synthetic mimotopes are used (Peltomaa et al., 2019a, 2017; Zou et al., 2016).

In this work, we have identified a mimotope for CPA from a commercial peptide library and developed a homogeneous immunoassay based on the synthetic mimotope. For the UC-RET-based competitive immunoassay, streptavidin (SA)-modified UCNPs ($NaYF_4$:Yb^{3+}, Er^{3+}) were coupled to the biotinylated mimotope and used as the energy donor, whereas the anti-CPA antibody fragment was conjugated to Alexa Fluor 555 (AF555) which functioned as the energy acceptor. The single-step assay could be used for the detection of CPA in maize samples in just 5 min. Contrary to time-consuming heterogeneous immunoassays with multiple steps and long incubation times, homogeneous immunoassays allow a rapid, single-step detection of analytes (Takkinen and Žvirblienė, 2019; Ni et al., 2021; Arai et al., 2021). To the best of our knowledge, the isolated peptide is the first reported mimotope for CPA, and the implemented assay is the first homogeneous immunoassay based on UCNPs and mimotopes to detect any mycotoxin.

2. Materials and methods

2.1. Materials

The Ph.D.-C7C phage display peptide library and the *Escherichia coli* ER2738 were purchased from New England Biolabs (Ipswich, MA, USA) and CPA from Cayman Chemical Company (Michigan, MI, USA). LB medium and agar granulated were provided by NZYtech (Lisbon, Portugal). Isopropylthio-β-galactoside (IPTG), 5-bromo-4-chloro-3-indolyl-β-D-galactopiranoside (X-Gal), 3,3′,5,5′-tetramethylbenzidine substrate (TMB), Tween-20, bovine serum albumin (BSA), MaxiSorp 96-

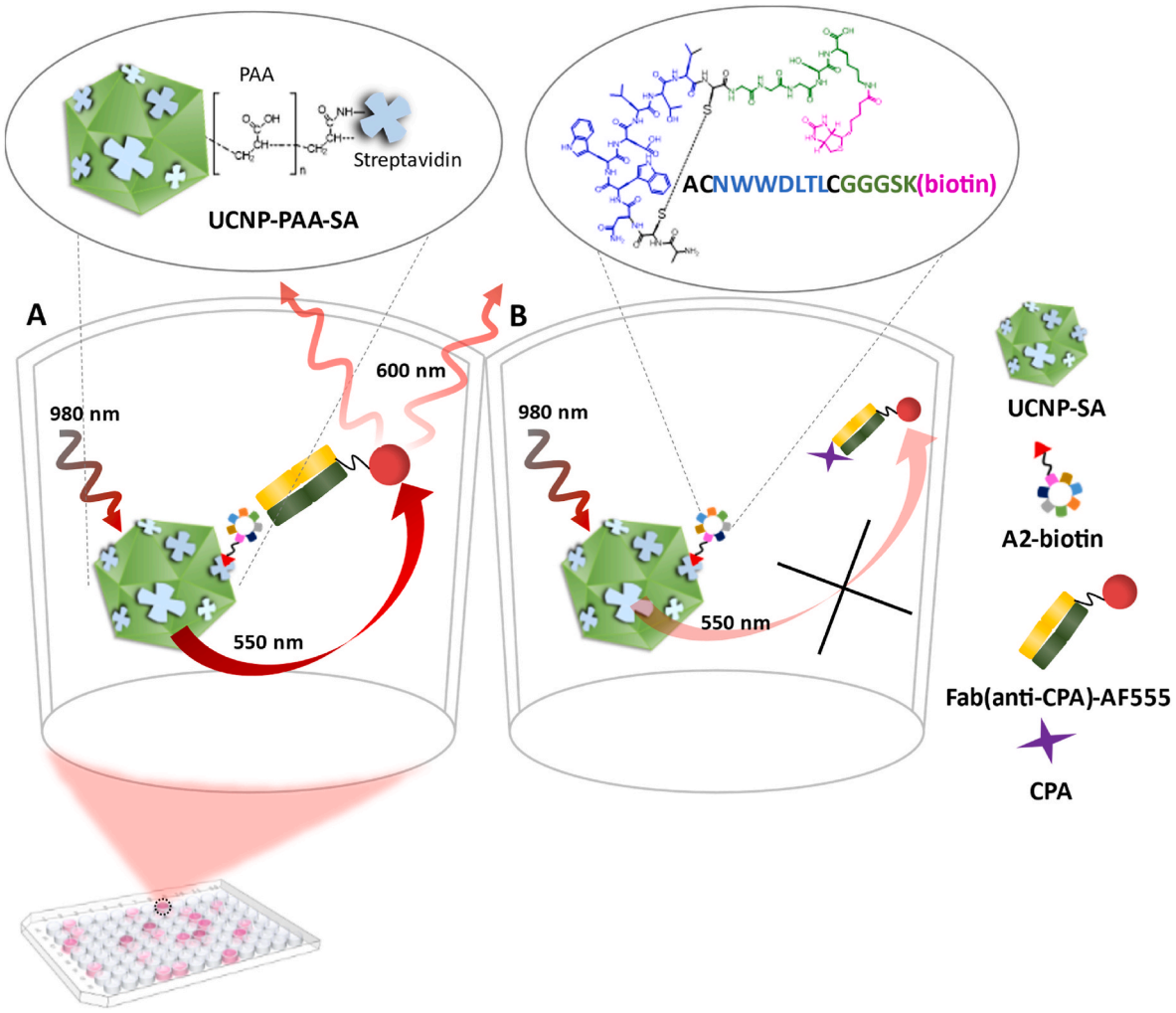

Fig. 1. Scheme of the homogeneous competitive UC-RET based immunoassay for the detection of CPA in one incubation step with no or low concentrations of CPA (A) and for high concentrations of CPA (B).

well Nunc immunoplates, methanol HPLC grade, and Pierce Mouse IgG1 Fab and F(ab')2 Preparation Kit were from Thermo Fisher Scientific (Waltham, MA, USA). Sera-Mag SpeedBeads Neutravidin-Coated Magnetic Particles, NAP-5 and NAP-10 columns were purchased from Cytiva (Chicago, IL, USA). Biotinylated synthetic mimotopes (AC $(X)_7$C-GGGSK (Biotin)-NH_2) were obtained from Peptide Synthetics (Fareham, UK). Horseradish peroxidase (HRP)-conjugated anti-M13 antibody was from Santa Cruz Biotechnology (Dallas, TX, USA), Peroxidase AffiniPure Rabbit Anti-Mouse IgG (H+L) from Jackson ImmunoResearch Inc. (West Grove, PA, USA) and Alexa Fluor® 555 succinimidyl ester from Molecular Probes, Invitrogen (Thermo Fisher Scientific Inc.). Assay buffer (50 mM TrisHCl, pH 7.75; 0.9% NaCl; 0.5% bovine serum albumin; 0.01% Tween 40; 0.05% NaN_3; 0.05% bovine gamma-globulin; 20 μM diethylenetriaminepentaacetic acid) was provided by Kaivogen (Turku, Finland), and Costar 96-well half-area black plates were by Corning Inc. (New York, NY, USA). Anti-CPA monoclonal antibody (mAb-1418) was provided by C. M. Maragos (Department of Agriculture, Peoria, IL, USA). Maize samples were purchased from local supermarkets in Turku, and they were confirmed to be free of CPA by HPLC-DAD, as described in the **Supplementary information**.

2.2. Selection of CPA-mimotopes by phage display

CPA mimotopes were selected by phage display from a commercial library consisting of 7-residue randomized peptide sequences displayed in a loop-shaped form (Ph.D.-C7C). The anti-CPA monoclonal antibody (mAb-1418) was used as the target. The panning rounds were performed as previously described (Peltomaa et al., 2020). Briefly, a total of three rounds were held for the selection of CPA mimotopes. A pre-selection step against BSA was carried out to eliminate non-specific phages prior to the actual selection with mAb-1418 in each round. The number of input phages (2×10^{11} pfu) was kept constant in all rounds. After the negative selection, the phage solutions were transferred to the mAb-1418 coated wells and incubated. The unbound phages were rinsed, and the remaining bound phages were eluted and subsequently amplified to start a new selection round. For the first round, the elution was done with 0.2 M glycine-HCl (pH 2.2), whereas a competitive elution step with free CPA was used in the second (100 ng mL^{-1} CPA) and third (10 ng mL^{-1} CPA) rounds. The second and third elution solutions were used to infect *E. coli* bacteria, and several individual plaques (clones) were selected from LB/IPTG/X-gal plates and amplified following a previously described method (Luque-Uría et al., 2021). The amplified phage clones were tested in the phage-based ELISA to select positive clones binding to the target antibody (protocol in **Supplementary information**). The positive clones were sequenced, and synthetic peptides based on these sequences were further tested in synthetic peptide-based ELISA (**Supplementary information**). The antibody interaction with the selected mimotope for the assay was confirmed by NMR as described in the **Supplementary information**.

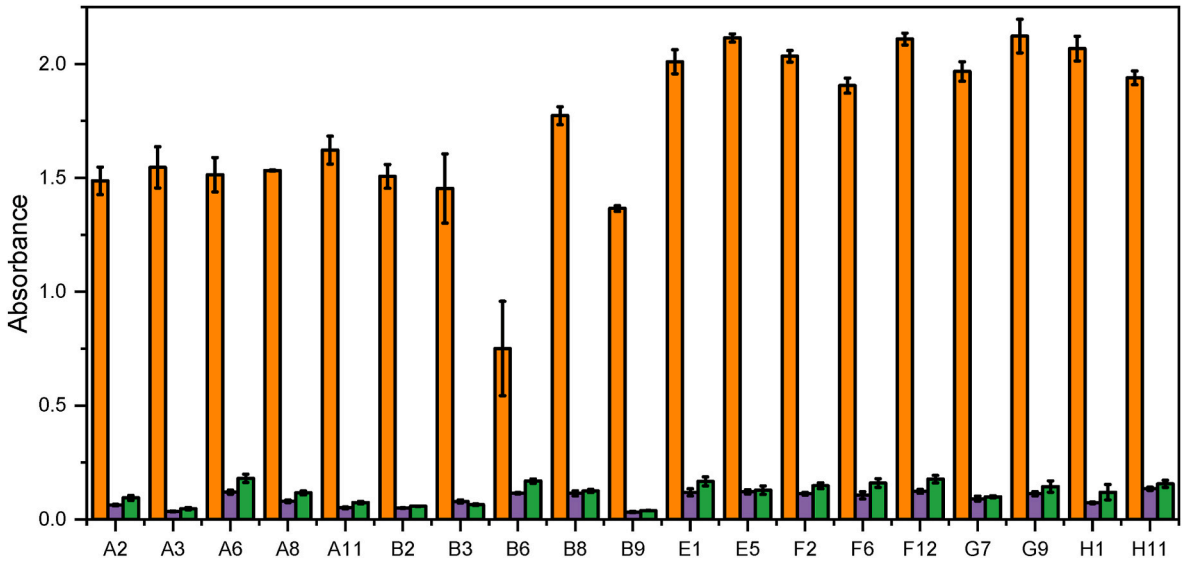

Fig. 2. Competitive phage-based ELISA with the 19 individual phage clones selected from rounds 2 and 3. Binding to the antibody in the absence of CPA (orange) was seen as high signals, and the competition in the presence of 100 ng mL^{-1} CPA (purple) resulted in low signals, similar to the background binding (no antibody; green). The phage dilution for all the clones was 1:20 from the stocks. The results are shown as the average absorbance values ± the standard deviation of the mean ($n = 3$).

2.3. Homogeneous UC-RET-based immunoassay

The homogeneous immunoassay (Fig. 1) was based on UC-RET between UCNPs and AF555 fluorophores. UCNPs were conjugated with streptavidin for capturing the biotinylated mimotope, and the AF555 was coupled with the anti-CPA antibody fragment, as described in the **Supplementary information**. The optimized homogeneous assay was performed in 96-well half-area black plates in a single step by mixing the final concentration 25 nM biotinylated mimotope A2, 7.5 μg mL^{-1} UCNP-SA, 6 nM Fab (anti-CPA)-AF555 and the sample (*i.e.*, sample extract or CPA standard solution) in a total volume of 80 μL in assay buffer. The wells were incubated for 5 min at room temperature with slow shaking, and the sensitized emission of the acceptor (AF555) was measured at 600 nm (with a bandpass filter 600/40 nm) upon excitation of the UCNP in the near-infrared at 980 nm using a modified Plate Chameleon microplate reader (Sedlmeier et al., 2016) (Hidex; Turku, Finland).

2.4. Sample preparation

A solid–liquid extraction was conducted to extract CPA from maize samples as previously described (Hossain et al., 2019; Maragos et al., 2017). First, 1 g of maize flour was weighed in a 15-mL centrifuge tube and extracted with 5 mL of methanol–water (80:20, v/v) for 1 h at RT with vigorous shaking (300 rpm). Samples were then centrifuged for 10 min at 6000 g, and aliquots of 1 mL were transferred to 2-mL centrifuge tubes and centrifuged again (5 min, 6000 g) to remove the solid matrix. Finally, the extracts were diluted 10-fold in the assay buffer to avoid potential matrix effects.

2.5. Data analysis

The measured signals were analyzed with OriginPro 2021 software (OriginLab Corp.) to obtain the toxin dose-response curve using a four-parameter logistic regression (4-PL).

$$y = A_{min} + \frac{A_{max} - A_{min}}{1 + \left(\frac{x}{IC_{50}}\right)^{b}} \quad (1)$$

where A_{min} is the asymptotic minimum and A_{max}, the asymptotic maximum (*i.e.*, the signal in the presence of the highest concentration of CPA and the absence of the toxin, respectively), b is the slope of the curve and IC_{50} the concentration of the analyte at the inflection point of the curve. The limit of detection (LOD) was determined using the average blank signal minus 3 times the standard deviation of the blank and the value was then interpolated into the four-parameter logistic dose-response curve. The dynamic range of the assay was defined as the CPA concentration that corresponds to the 20%–80% inhibition (IC_{20}–IC_{80}).

3. Results and discussion

3.1. Selection of CPA mimotopes

CPA mimotopes were selected from a commercial phage library displaying random sequences of 7 amino acids in a constrained loop shape (Ph.D.-C7C). The protocol aimed to increase the specificity of the mimotope towards the paratope of the anti-CPA antibody mAb-1418 over the three panning rounds. In the first round, the three wells with a high concentration of immobilized antibody were used to provide a large surface area to bind the highest number of phage-displayed peptides from the initial pool of 2×10^{9} different clones. In the subsequent rounds, the stringency for the selection was increased, and the amount of antibody was reduced to favor the selection of high affinity binders. On the other hand, increasing the number of washes and the percentage of Tween-20 in the washing buffer aimed to remove non-specifically bound peptides. Finally, the competitive CPA-based elution in rounds two and three allowed the collection of clones unequivocally interacting with the same antibody binding site as CPA. Enrichment of the eluted phages after each round was observed together with increased signal-to-background ratios in the phage-based ELISA (Fig. S1).

Several individual phage clones from the second and third rounds were selected and assessed in monoclonal phage-based ELISAs. The success in selecting CPA mimotopes was confirmed since 82% of the clones (28 out of 34) showed specific binding to the antibody (Fig. S2). A total of 19 individual phages with the best signal-to-background ratios were successfully assayed in competitive ELISAs (Fig. 2). DNA sequencing of these 19 clones revealed four different peptide sequences: AC**NWWDLTL**C (named **A2**; 6 out of 19 sequences peptides), AC**TWWDMAF**C (named **A6**; 4 out of 19), AC**VWWDHTY**C (named

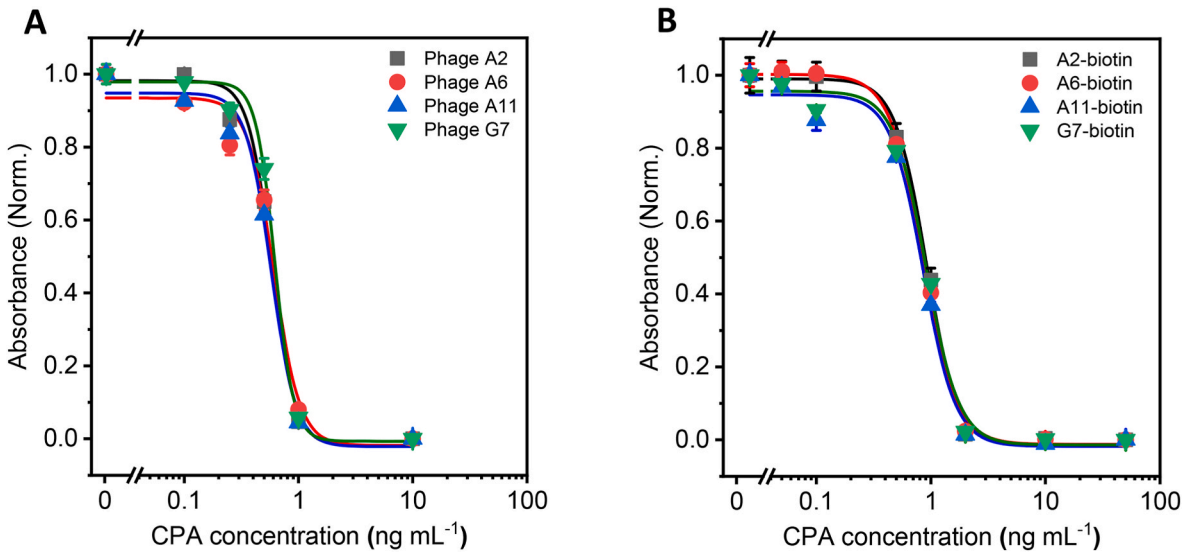

Fig. 3. Competitive (A) phage-based ELISAs and (B) synthetic peptide-based ELISA using the four different mimotopes (named A2, A6, A11, and G7) with different concentrations of free CPA. The results are shown as the average normalized absorbance values ± the standard deviation of the mean ($n = 3$).

A11; 8 out of 19) and AC**EWWDVTY**C (named **G7**; 1 out of 19). Interestingly, the amino acid motif WWD was observed in all of those sequences suggesting its importance for the epitope mimicking nature of the peptide. Saturation transfer difference (STD) NMR experiments confirmed that the aromatic tryptophan residues of the mimotope A2 were interacting with the antibody (Fig. S3).

Calibration plots were performed at concentrations of CPA ranging between 0 and 10 ng mL^{-1} (Fig. 3a) with the phage-displayed peptides with the four different sequences. No significant differences between the peptides were observed in terms of sensitivity (LOD and IC_{50}) and dynamic range (IC_{20}–IC_{80}) (Table S1).

To confirm the peptide binding independent of the phage, biotinylated peptides were synthetized with an N-terminal biotin which allows easy coupling of the peptide. The synthetic peptide-based ELISA using neutravidin-coupled magnetic beads demonstrated that the mimotopes were able to recognize the antibody paratope and compete against free CPA for the binding sites even in the absence of the phage (Fig. 3b). As in the case of the phage-based ELISA, negligible differences were observed between the different mimotopes for the concentration values assessed in the synthetic peptide-based assay (Table S1). Both phage-based and synthetic peptide-based (phage-free) ELISAs provided calibration plots with a very narrow dynamic range. The use of the synthetic mimotopes provided similar figures of merits compared to the phage-based assay (Table S1).

3.2. Analysis of the peptide-binding kinetics by SPR

Surface plasmon resonance (SPR) measurements were performed to compare the binding properties of the four mimotopes (synthetic biotinylated mimotopes) isolated by phage display and the CPA with the target anti-CPA mAb-1418 monoclonal antibody. SPR is a molecular size-dependent methodology and due to the low molecular weight of CPA (336.4 g mol^{-1}), the binding kinetics of free CPA could not be studied. Therefore, a conjugate of CPA with β-lactoglobulin (Maragos et al., 2017) (CPA-BLG, MW: 18.4 kDa approximately) was used as the analyte to investigate the affinity of the toxin for mAb-1418, which was captured by an anti-mouse IgG covalently immobilized on the chip surface. For the same reason, the study of the binding kinetics of biotinylated mimotopes (MW between 1834 and 1893 g mol^{-1}) could not be performed in the same format as the CPA-BLG (SPR protocols in **Supplementary information**) and an anti-biotin IgG was covalently immobilized on the chip surface and used to capture the biotinylated mimotopes. The mAb-1418 was passed through the chip as the analyte in this case.

All four mimotopes showed such fast peptide−antibody dissociation rates (Figs. S4a–S4d) that it was impossible to calculate affinity constants by kinetic fitting. However, according to the binding level for the same capture level of the peptides (6 RU approximately) and at a fixed concentration of the analyte (mAb-1418, 4 μM), A2-biotin showed the best affinity for the antibody as it reported the highest response (RU, Fig. S4e). Regarding the dissociation rates obtained for all the mimotopes, A2-biotin was selected as the most suitable competitor due to its superior binding properties for the antibody. This way, more sensitive assays can be achieved as a lower concentration of the selected peptide is preferred to obtain a lower IC50 value in the assay. At the antibody concentration levels assayed (0−4 μM), an affinity fitting (Langmuir equilibrium fit) provided an affinity value for A2-biotin in the micromolar range.

The mycotoxin (as CPA-BLG conjugate) showed an affinity constant of 0.8 nM, as a result of the division of the dissociation constant ($k_{off} = 4.64 \cdot \times 0.10^{-4}\ s^{-1}$) and the association constant ($k_{on} = 5.83 \cdot \times 10^{5}\ M^{-1}\ s^{-1}$). In this case, the antibody−mycotoxin dissociation rate (Fig. S4f) was much lower than with the peptides. The affinity constant of CPA-BLG and the lower dissociation rate observed demonstrated the higher affinity of the antibody for the mycotoxin-conjugate than for the mimotope, which may be relevant to obtain more sensitive assays using the peptide competitor (Peltomaa et al., 2017).

3.3. Homogeneous UC-RET-based immunoassay optimization

Rapid techniques for mycotoxin analysis have become increasingly significant. Therefore, we developed a simple homogenous UC-RET-based immunoassay using the novel mimotopes. As the energy transfer is conditioned by the spectral overlap between the emission of the donor and the excitation of the acceptor and the donor–acceptor distance (Takkinen and Žvirblienė, 2019), we chose AF555 as the acceptor taking advantage of the high emission of the $NaYF_4$:Yb^{3+}, Er^{3+} UCNP at 550 nm (Fig. S5) Furthermore, to reduce the distance between the donor and the acceptor in this immunoassay, the fragment antigen binding (Fab) of anti-CPA antibody was used instead of the intact IgG.

$NaYF_4$:Yb^{3+}, Er^{3+} UCNPs (particle size 27.3 nm, Fig. S6) (Palo et al., 2017; Raiko et al., 2021) were functionalized with streptavidin, and the functionality of the conjugates in the energy transfer was checked in a biotin-based competitive assay (Fig. S7). Similar chemistry was applied

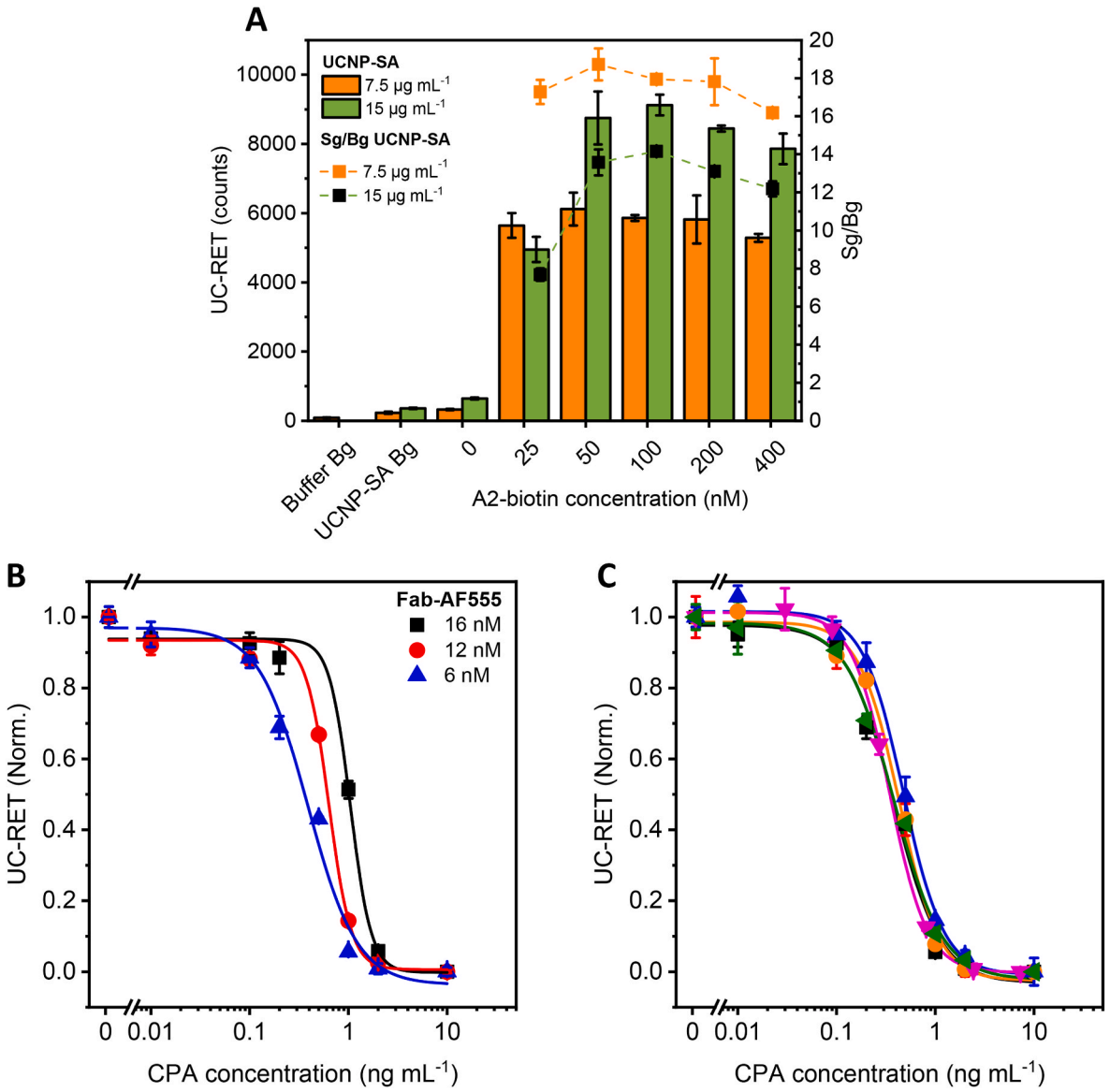

Fig. 4. Optimization of the homogeneous UC-RET immunoassay. (A) Optimization of A2-biotin and UCNP-SA concentrations (Fab-AF555 16 nM); (B) evaluation of the sensitivity of the assay with different concentrations of Fab-AF555 (A2-biotin 25 nM and UCNP-SA 7.5 μg mL^{-1}) and (C) optimization of the assay format. Incubation of UCNP-SA + A2-biotin for 20 min and Fab-AF555 + free CPA for 5 (A-5, ■), 15 (A-15, ●) and 30 min (A-30, ▲), Fab-AF555 + free CPA + A2-biotin for 10 min and UCNPs-SA for 10 min (B, ▼) and UCNP-SA + Fab-AF555 + free CPA + A2-biotin for 5 min (C, ◀). The results are shown as the average fluorescence values or normalized signals values ± the standard deviation of the mean ($n = 3$).

to conjugate the anti-CPA Fab to Alexa Fluor 555 (Fab-AF555) (Akter and Lamminmäki, 2021) *via* NHS esters of the dye and primary amino groups of the Fab. The labeling ratio of the Fab-AF555 was estimated to be approximately 1:1 (*i.e.*, one molecule of dye per molecule of Fab). Some authors have reported that high labeling degrees can lead to a self-quenching of the fluorescence of the dyes (Rantanen et al., 2007). Other authors (Blomberg et al., 1999) found an optimal labeling degree of 2–5 Alexa546 molecules per IgG molecule for an energy transfer application. The anti-CPA Fab used in this work is 3 times smaller than the IgG molecule, suggesting an optimal labeling degree to be close to 1. Therefore, the labeling ratio obtained was considered adequate to ensure the UC-RET avoided the self-quenching of the AF555.

The UCNP-SA-conjugates were used to bind the biotinylated mimotope which competes with the free CPA for the binding sites of the Fab-AF555 (Fig. 1). In the absence or at low concentrations of the toxin, the Fab-AF555 binds to the mimotope allowing the UC-RET. At high concentration of CPA, the Fab-AF555 binds to the free mycotoxin and no UC-RET is observed due to the large donor–acceptor distance. The optimization of the concentration of the components involved in the UC-RET homogeneous assay was critical due to the absence of washing steps. Therefore, an optimization of the concentrations of UCNP-SA, A2-biotin and Fab-AF555 was conducted. Various concentrations of the mimotope A2-biotin (1.56−200 nM) were tested, and the highest signals were obtained with 50 nM A2-biotin (Fig. S8). Furthermore, different concentrations of the biotinylated mimotope (25–400 nM) were assayed with two concentrations of UCNP-SA (7.5 and 15 μg mL^{-1}) in order to check that there was no excess of the mimotope in solution which might decrease the UC-RET (Fig. 4a). Similar signals were obtained with 25 nM of A2-biotin for both concentrations of UCNP-SA, demonstrating that this concentration is optimal for 7.5 mg mL^{-1} UCNP-SA. As it also resulted in better Sg/Bg ratios than 15 μg mL^{-1} UCNP-SA, 25 nM A2-biotin with 7.5 mg mL^{-1} UCNP-SA were selected as the optimal concentrations for the assays.

A slight decrease in signal was observed with increasing excess of

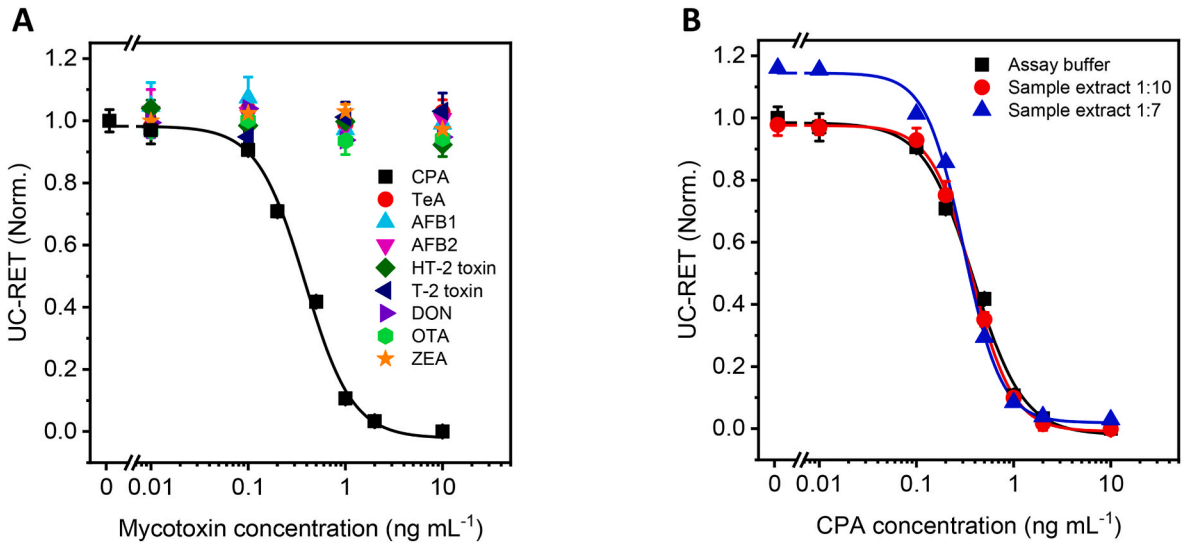

Fig. 5. (A) Calibration plot of the optimized homogeneous UC-RET immunoassay for the detection CPA and cross-reactivity analysis with other mycotoxins commonly found in maize. (B) Evaluation of the matrix effect with different dilutions of maize extracts. The results are shown as the average normalized signals ± the standard deviation of the mean ($n = 3$).

biotinylated mimotope for a fixed amount of UCNP-SA and Fab-AF555 (Fig. S8 and Fig. 4a), which could be attributed to the Fab-AF555 being in excess. For this reason, different concentrations of Fab-AF555 (1.4–16 nM) were tested with the optimized amounts of UCNP-SA and A2-biotin (Fig. S9). It would be expected that if there was an excess of Fab-AF555, slightly lower concentrations of the conjugated antibody fragment would provide comparable signals (Lahtinen et al., 2016). Nevertheless, this did not occur, and a large signal decrease was observed even with the next lower concentration of Fab-AF555 tested. This means that the interaction between the mimotope and the anti-CPA Fab is conditioned by their affinity, and that higher concentrations of Fab-AF555 enhance their interaction. The highest signal and Sg/Bg ratio were obtained with 16 nM Fab-AF555, but the effect on the assay sensitivity was studied more in depth by performing calibration curves (CPA 0–10 ng mL^{-1}) with different concentrations of Fab-AF555 (Fig. 4b and Fig. S10). The lower the Fab-AF555 concentration was used, the better the sensitivity of the assay (in terms of IC_{50}), even though decreasing the Fab-AF555 concentration also provided lower signals and Sg/Bg ratios. The highest sensitivity and the widest dynamic range were obtained with a final concentration of 6 nM Fab-AF555 which was selected for the optimized homogeneous assay.

Different incubation times and orders of reagent addition were tested (Fig. 4c). First, an assay with two separate incubation steps was carried out (A). UCNP-SA and A2-biotin were first incubated for 20 min and then the Fab-AF555 and free CPA were added and incubated for 5 (A-5), 15 (A-15) or 30 min (A-30) before the measurement. Longer incubation times in the second step resulted in less sensitive assays with narrower dynamic ranges. Secondly, another immunoassay was performed (B) but with a pre-incubation of Fab-AF555, free CPA and A2-biotin for 10 min to establish the competition. UCNP-SA was then added, and the mixture was incubated for 10 min more. Finally, a one-step assay was conducted (C) in which all components were mixed and incubated together for 5 min. Assay formats B and C provided comparable sensitivity to the A-5 format. The lowest limit of detection and the largest dynamic range were obtained for A-5 and C formats. Due to the short incubation time and the simplicity of the assay, in addition to the analytical features provided, the one-step assay (C) was selected as the optimal assay format. Different incubation times of the 1-step assay were also evaluated but they did not improve analytical characteristics (Fig. S11).

3.4. Assay characterization

The optimized homogeneous UC-RET-based immunoassay was performed in a single step by incubating UCNP-SA, A2-biotin, Fab-AF555 and the sample for 5 min in a total volume of 80 μL. The fluorescence signal was obtained by resonance energy transfer from the UCNPs. The calibration plot obtained for the analysis of CPA (0–10 ng mL^{-1}) in the assay buffer is depicted in Fig. 5a. The immunoassay showed suitable analytical features with an IC_{50} value of 0.36 ± 0.08 ng mL^{-1} and an inter-day relative standard deviation (RSD) of 9% ($n = 3$). The LOD obtained in the assay buffer was 30 pg mL^{-1}, and the dynamic range (IC_{20}–IC_{80}) was from 0.15 ± 0.05 to 0.9 ± 0.2 ng mL^{-1}. As can be seen in Table S2, this homogeneous immunoassay presents better analytical characteristics than the phage-based and synthetic mimotope-based heterogeneous assays described in this work.

Moreover, in comparison with other immunoassays reported for the detection of CPA, the homogeneous UC-RET has several advantages which are summarized in Table S2. The heterogeneous ELISAs for CPA are time-consuming and require conjugation of the toxin to a carrier protein (*e.g.* BSA or HRP) (Yu and Chu, 1998; Maragos et al., 2017). The use of mimotopes avoids the toxin conjugation step and the mimotope-based UC-RET also results in better sensitivity than the heterogeneous ELISA using the same antibody (Maragos et al., 2017). Imaging surface plasmon resonance (iSPR), a novel variant of traditional SPR, was applied to the monitoring of CPA (Hossain et al., 2019). However, association, amplification and dissociation steps were needed for each analysis, which significantly increased the detection time. The lateral flow immunoassay (Li et al., 2020) only allowed qualitative detection of CPA and required significantly longer assay time than the UC-RET assay which is the fastest immunoassay described for the analysis of CPA thus far, reporting the results in only 5 min.

3.5. Cross-reactivity

The selectivity of the immunoassay was evaluated in cross-reactivity assays with other common mycotoxins reported worldwide (structures in Fig. S12) and co-produced by the same fungi species (*A. flavus*), such as aflatoxins B_1 (AFB_1) and B_2 (AFB_2) or produced by other fungi species but usually found in maize, such as tenuazonic acid (TeA), HT-2 and T-2 toxins, deoxynivalenol (DON), ochratoxin A (OTA) and zearalenone (ZEA) (Fig. 5a). No cross-reactivity was observed with any of the

Table 1
Analysis of CPA in maize samples with the UC-RET immunoassay and HPLC-DAD.

Sample	Spiked CPA(μg kg^{-1})	UC-RET immunoassay			HPLC-DAD		
		Measured (μg kg^{-1})	Recovery (%)	RSD (%)	Measured (μg kg^{-1})	Recovery (%)	RSD (%)
1	–	< LOD	–	–	< LOD	–	–
2	–	< LOD	–	–	< LOD	–	–
3	–	< LOD	–	–	< LOD	–	–
4	5	4.6	93	4	4.4	88	7
5	10	8.9	89	9	9.4	94	4
6	20	19.2	96	5	17.8	89	9
7	40	42.0	105	7	39.6	99	6
8	80	77.6	97	15	79.2	99	3
9	160	186.2	116	7	152.1	95	3

mycotoxins studied, demonstrating the selectivity of the antibody for CPA. It is essential to highlight the absence of cross-reactivity especially with AFB_1 and AFB_2, as CPA commonly co-occurs with these aflatoxins in maize samples (Ostry et al., 2018).

3.6. Sample analysis

The optimized immunoassay was applied to the analysis of maize samples. Calibration curves (CPA 0–10 ng mL^{-1}) in both assay buffer and sample extract were carried out to evaluate the matrix effect (Fig. 5b). CPA-free maize samples were extracted with MeOH:water (80/20, v/v) and, after a centrifugation step, the supernatant was diluted in assay buffer. Matrix-matched calibration plots were performed with different dilutions of the extracts, and no matrix effect was observed for a 10-fold dilution of the sample extract, resulting in a limit of detection (LOD) of 1.5 μg kg^{-1} in maize. The LOD obtained was better than those previously reported in the literature (Hossain et al., 2019; Li et al., 2020; Yu and Chu, 1998).

Three different maize samples were purchased from local markets, and they were confirmed to be free of CPA by HPLC-DAD. Analysis with the immunoassay was carried out but also no CPA was found above the limit of detection of the assay. However, this mycotoxin has been reported in several maize samples at much higher concentration levels from 8.1 to 2998 μg kg^{-1} (Hossain et al., 2019; Maragos et al., 2017; Yu and Chu, 1998) than the LOD obtained in this assay. Therefore, the immunoassay is able to detect frequent concentrations of CPA in naturally contaminated samples. The assay was also applied to the analysis of maize samples spiked with different concentrations of CPA ranging from 5 to 160 μg kg^{-1} (Table 1). The applicability of the immunoassay was demonstrated with recoveries ranging between 93 and 116% with a relative standard deviation lower than 15%. These results were confirmed by HPLC-DAD analysis as described in the **Supplementary information**.

4. Conclusions

Phage display has been confirmed as a powerful tool for the selection of CPA mimotopes for the development of competitive immunoassays, avoiding the need for toxin-conjugates. SPR measurements revealed a suitable affinity of the antibody to the mimotope which allows more sensitive assays. Consequently, the immunoassay developed provided a higher sensitivity than the majority of immunoassays described in the literature, even more sensitive than an ELISA using the same monoclonal antibody (Maragos et al., 2017). Furthermore, the assay reported in this work is the first homogeneous immunoassay for the detection of CPA and also the first homogeneous UC-RET-based immunoassay for the detection of any mycotoxin. We also applied this novel method to the analysis of spiked maize samples, achieving a lower LOD than those reported in the literature (Table S2). Although there is still no legislation for the maximum residue levels of CPA in foodstuffs, the LOD obtained (1.5 μg kg^{-1}) is adequate to detect this toxin at the levels at which it is usually found in maize. The applicability of UCNPs in homogeneous immunoassays has proven to be one of the fastest immunoassays described in the literature, providing reliable analytical results in just 5 min. The proposed UC-RET-based assay, combining the CPA mimotope-coupled UCNP photon donor and the acceptor AF555 tagged anti-CPA Fab, showed great promise as a rapid screening method to analyze CPA contamination in foodstuffs, and it could be further developed in the future to test for other mycotoxins or additional contaminants.

Disclaimer

Mention of trade names or commercial products in this publication is solely for the purpose of providing specific information and does not imply recommendation or endorsement by the US Department of Agriculture. USDA is an equal opportunity provider and employer.

CRediT authorship contribution statement

Fernando Pradanas-González: Conceptualization, Methodology, Data curation, Writing – original draft. **Riikka Peltomaa:** Conceptualization, Methodology, Writing – review & editing. **Satu Lahtinen:** Conceptualization, Methodology, Data curation, Writing – review & editing. **Álvaro Luque-Uría:** Methodology, Writing – review & editing. **Vicente Más:** Methodology. **Rodrigo Barderas:** Writing – review & editing. **Chris M. Maragos:** Conceptualization, Methodology, Writing – review & editing. **Ángeles Canales:** Methodology. **Tero Soukka:** Conceptualization, Methodology, Supervision, Writing – review & editing, Funding acquisition. **Elena Benito-Peña:** Conceptualization, Methodology, Supervision, Writing – review & editing. **María C. Moreno-Bondi:** Conceptualization, Methodology, Supervision, Funding acquisition.

Declaration of competing interest

The authors declare that they have no known competing financial interests or personal relationships that could have appeared to influence the work reported in this paper.

Data availability

Data will be made available on request.

Acknowledgements

This work has been funded by the Ministry of Science, Innovation and Universities (MSIU) (RTI2018-096410-B-C21, PID2021-127457OB-C21 and PID2019-105237 GB-I00). FP acknowledges the MSIU for an FPU contract.

Appendix A. Supplementary data

Supplementary data to this article can be found online at https://doi.

org/10.1016/j.bios.2023.115339.

References

Abdul Hakeem, D., Su, S., Mo, Z., Wen, H., 2021. Crit. Rev. Food Sci. Nutr. 1–42.
Akter, S., Lamminmäki, U., 2021. Anal. Bioanal. Chem. 413, 6159–6170.
Ansari, P., Häubl, G., 2016. Food Chem. 211, 978–982.
Ansari, A.A., Thakur, V.K., Chen, G., 2021. Coord. Chem. Rev. 436, 213821.
Arai, S., Camargo, M., de, A.S.S., 2021. Nanoscale Adv. 3, 5135–5165.
Aresta, A., Cioffi, N., Palmisano, F., Zambonin, C.G., 2003. J. Agric. Food Chem. 51, 5232–5237.
Blomberg, K., Hurskainen, P., Hemmilä, I., 1999. Clin. Chem. 45, 855–861.
Burdock, G.A., Flamm, W.G., 2000. Int. J. Toxicol. 19, 195–218.
De Waal, E.J., 2002. Int. J. Toxicol. 21, 425–427.
Dong, H., Sun, L.-D., Yan, C.-H., 2015. Chem. Soc. Rev. 44, 1608–1634.
Farka, Z., Jurík, T., Kovář, D., Trnková, L., Skládal, P., 2017. Chem. Rev. 117, 9973–10042.
Fu, X., Chen, L., Choo, J., 2017. Anal. Chem. 89, 124–137.
Gorris, H.H., Resch-Genger, U., 2017. Anal. Bioanal. Chem. 409, 5875–5890.
Hahnau, S., Weiler, E.W., 1991. J. Agric. Food Chem. 39, 1887–1891.
Hahnau, Sabine, Weiler, E.W., 1993. J. Agric. Food Chem. 41, 1076–1080.
He, Q., Xu, Y., Zhang, C., Li, Y., Huang, Z., 2014. Food Control 39, 56–61.
Hossain, Z., Busman, M., Maragos, C.M., 2019. Anal. Bioanal. Chem. 411, 3543–3552.
Hou, S., Ma, Z., Meng, H., Xu, Y., He, Q., 2019. Talanta 194, 919–924.
Hu, X., Zhang, P., Wang, D., Jiang, J., Chen, X., Liu, Y., Zhang, Z., Tang, B.Z., Li, P., 2021. Biosens. Bioelectron. 182, 113188.
Huang, Xuan, Chu, F.Sun, 1993. J. Agric. Food Chem. 41, 329–333.
Huang, D.-T., Fu, H.-J., Huang, J.-J., Luo, L., Lei, H.-T., Shen, Y.-D., Chen, Z.-J., Wang, H., Xu, Z.-L., 2021. J. Agric. Food Chem. 69, 11743–11752.
Hymery, N., Masson, F., Barbier, G., Coton, E., 2014. Toxicol. Vitro 28, 940–947.
Jia, M., Liao, X., Fang, L., Jia, B., Liu, M., Li, D., Zhou, L., Kong, W., 2021. TrAC, Trends Anal. Chem. 136, 116193.
Lahtinen, S., Wang, Q., Soukka, T., 2016. Anal. Chem. 88, 653–658.
Li, Y., Liu, L., Kuang, H., Xu, C., 2020. J. Food Sci. 85, 105–113.
Lin, X., Yu, W., Tong, X., Li, C., Duan, N., Wang, Z., Wu, S., 2022. Crit. Rev. Anal. Chem. 1–34.
Luque-Uría, Á., Peltomaa, R., Nevanen, T.K., Arola, H.O., Iljin, K., Benito-Peña, E., Moreno-Bondi, M.C., 2021. Anal. Chem. 93, 10358–10364.
Ma, X., Ye, Y., Sun, J., Ji, J., Wang, J.-S., Sun, X., 2022. J. Agric. Food Chem. 70, 5166–5176.
Maragos, C.M., Sieve, K.K., Bobell, J., 2017. Mycotoxin Res. 33, 157–165.
Motta, S. da, Soares, L.M.V., 2001. Food Addit. Contam. 18 (7), 630–634.
Ni, Y., Rosier, B.J.H.M., van Aalen, E.A., Hanckmann, E.T.L., Biewenga, L., Pistikou, A.-M.M., Timmermans, B., Vu, C., Roos, S., Arts, R., Li, W., de Greef, T.F.A., van Borren, M.M.G.J., van Kuppeveld, F.J.M., Bosch, B.-J., Merkx, M., 2021. Nat. Commun. 12, 4586.
Ostry, V., Toman, J., Grosse, Y., Malir, F., 2018. World Mycotoxin J. 11, 135–148.
Palo, E., Tuomisto, M., Hyppänen, I., Swart, H.C., Hölsä, J., Soukka, T., Lastusaari, M., 2017. J. Lumin. 185, 125–131.
Peltomaa, R., López-Perolio, I., Benito-Peña, E., Barderas, R., Moreno-Bondi, M.C., 2016. Anal. Bioanal. Chem. 408, 1805–1828.
Peltomaa, R., Benito-Peña, E., Barderas, R., Sauer, U., González Andrade, M., Moreno-Bondi, M.C., 2017. Anal. Chem. 89, 6216–6223.
Peltomaa, R., Amaro-Torres, F., Carrasco, S., Orellana, G., Benito-Peña, E., Moreno-Bondi, M.C., 2018a. ACS Nano 12, 11333–11342.
Peltomaa, R., Benito-Peña, E., Moreno-Bondi, M.C., 2018b. Anal. Bioanal. Chem. 410, 747–771.
Peltomaa, R., Agudo-Maestro, I., Más, V., Barderas, R., Benito-Peña, E., Moreno-Bondi, M.C., 2019a. Anal. Bioanal. Chem. 411, 6801–6811.
Peltomaa, R., Benito-Peña, E., Barderas, R., Moreno-Bondi, M.C., 2019b. ACS Omega 4, 11569–11580.
Peltomaa, R., Fikacek, S., Benito-Peña, E., Barderas, R., Head, T., Deo, S., Daunert, S., Moreno-Bondi, M.C., 2020. Microchim. Acta 187, 547.
Peltomaa, R., Benito-Peña, E., Gorris, H.H., Moreno-Bondi, M.C., 2021. Analyst 146, 13–32.
Raiko, K., Lyytikäinen, A., Ekman, M., Nokelainen, A., Lahtinen, S., Soukka, T., 2021. Clin. Chim. Acta 523, 380–385.
Rantanen, T., Päkkilä, H., Jämsen, L., Kuningas, K., Ukonaho, T., Lövgren, T., Soukka, T., 2007. Anal. Chem. 79, 6312–6318.
Rantanen, T., Järvenpää, M.-L., Vuojola, J., Kuningas, K., Soukka, T., 2008. Angew. Chem. Int. Ed. 47, 3811–3813.
Rouf Shah, T., Prasad, K., Kumar, P., 2016. Cogent Food Agric. 2, 1166995.
Sedlmeier, A., Hlaváček, A., Birner, L., Mickert, M.J., Muhr, V., Hirsch, T., Corstjens, P.L. A.M., Tanke, H.J., Soukka, T., Gorris, H.H., 2016. Anal. Chem. 88, 1835–1841.
Smartt, A.E., Ripp, S., 2011. Anal. Bioanal. Chem. 400, 991–1007.
Soares, C., Rodrigues, P., Freitas-Silva, O., Abrunhosa, L., Venâncio, A., 2010. World Mycotoxin J. 3, 225–231.
Takkinen, K., Žvirblienė, A., 2019. Curr. Opin. Biotechnol., Analytical Biotechnology 55, 16–22.
Vulić, A., Lešić, T., Kudumija, N., Zadravec, M., Kiš, M., Vahčić, N., Pleadin, J., 2021. Food Control 123, 107814.
Wang, Y., Wang, H., Li, P., Zhang, Q., Kim, H.J., Gee, S.J., Hammock, B.D., 2013. J. Agric. Food Chem. 61, 2426–2433.
Wang, W., Zhang, Q., Ma, F., Li, P., 2022. Food Chem. 378, 132020.
Wilhelm, S., 2017. ACS Nano 11, 10644–10653.
Yan, J., Shi, Q., You, K., Li, Y., He, Q., 2019. J. Pharm. Biomed. Anal. 168, 94–101.
Yu, W., Chu, F.S., 1998. J. Agric. Food Chem. 46, 1012–1017.
Zou, X., Chen, C., Huang, X., Chen, X., Wang, L., Xiong, Y., 2016. Talanta 146, 394–400.